

Final Technical Report

Grant #: DE-FG03-99ER14943

Title: Membrane-organized Chemical Photoredox Systems

Principal Investigator: James K. Hurst
Department of Chemistry
Washington State University
Pullman, WA 99164-4630

Period covered: 08/07/2001—12/15/2005
Total project period: 04/01/2002—03/31/2006[†]

[†]includes 1 yr no-cost extension

A. Publications:[‡]

- (1) R. F. Khairutdinov & JKH: “Photocontrol of Ion Permeation through Bilayer Membranes using an Amphiphilic Spiropyran”, *Langmuir* **2001**, *17*, 6881-6886.
- (2) H. Yamada, T. Koike & JKH: “Water Exchange Rates in the Diruthenium μ -Oxo Ion, *cis,cis*-[(bpy)₂Ru(OH₂)]₂O⁴⁺”, *J. Am. Chem. Soc.* **2001**, *123*, 12775-12780.
- (3) R. F. Khairutdinov & JKH: “Cyclic Transmembrane Charge Transport Mediated by Pyrylium and Thiopyrylium Ions” *J. Am. Chem. Soc.* **2001**, *123*, 7352-7359.
- (4) H. Yamada, W. F. Siems, T. Koike & JKH: “Mechanisms of Water Oxidation Catalyzed by the *cis,cis*-[(bpy)₂Ru(OH₂)]₂O⁴⁺ Ion”, *J. Am. Chem. Soc.* **2004**, *126*, 9786-9795.
- (5) R. F. Khairutdinov & JKH: “Light Driven Transmembrane Ion Transport by Spiropyran—Crown Ether Supramolecular Assemblies”, *Langmuir* **2004**, *20*, 1781-1785.
- (6) JKH: “Water Oxidation Catalyzed by Dimeric μ -Oxo Bridged Ruthenium Diimine Complexes”, *Coord. Chem. Rev.* **2005**, *249*, 313-328 (invited review).
- (7) L. Zhu, M.-Q. Zhu, JKH & A. D. Q. Li: “Light-controlled Molecular Switches Modulate Nanocrystal Fluorescence”, *J. Am. Chem. Soc.* **2005**, *127*, 8968-8970.
- (8) L. Zhu, R. F. Khairutdinov, J. L. Cape & JKH: “Photoregulated Transmembrane Charge Separation by Linked Spiropyran-Anthraquinone Molecules”, *J. Am. Chem. Soc.* **2006**, *128*, 825-835.

- (9) M.-Q. Zhu, L. Zhu, J. J. Han, W. Wu, JKH & A. D. Q. Li: “Photochromic Polymer Nanoparticles with Optically Switchable Luminescence”, under revision for publication in *J. Am. Chem. Soc.*
- (10) L. Zhu, R. F. Khairutdinov & JKH: “Electroneutral Transmembrane e^-/OH^- Antiport by Low-potential Pyrylium Ions”, manuscript in preparation.

B. Progress Summary:

1. General Objectives

The overall project has had three main objectives, namely to develop: (1) water oxidation catalysts suitable for use in membrane-based integrated photochemical systems; (2) molecules capable of functioning as electroneutral transmembrane electron carriers for H_2 photoproduction; (3) membrane-organized electrogenic transmembrane redox systems whose reaction rates and pathways can be modulated by light.

2. Water Oxidation Catalysts (objective 1)

a. Published Work (manuscripts 2,4,6)

It is now widely accepted that technologically attractive methods for large-scale photoproduction of H_2 from water or removal of greenhouse gases by photoreduction will probably require water as the source of electrons. Recognition of this requirement has prompted renewed interest in the development of water oxidation catalysts [1]. The most extensively studied homogeneous catalysts for water oxidation are the *cis,cis*- $[(bpy)_2Ru^{III}(OH_2)]_2O^{4+}$ ions originally described by T. J. Meyer and associates [2] and related homologs containing substituted bipyridine ligands. However, despite extensive investigations in several laboratories, the reactivities of these ions are still poorly understood, with issues such as the identities of detectable reaction intermediates, the rate-limiting steps in catalytic cycles, assignment of the O_2 -evolving species, and the

mechanism of O-O bond formation remaining unresolved. Historically, a major impediment to characterizing the reaction mechanism has been the inability to isolate the complex in its higher oxidation states in pure form. We have recently overcome this problem by employing a carbon fiber columnar flow electrode to carry out rapid bulk electrolysis [3]. The key feature of this flow-through electrode is an extremely large surface area/unit volume ($\sim 1500 \text{ cm}^2/\text{mL}$) which allows efficient oxidation to a preset potential with minimum residence time of the complex within the electrode. Effluent solutions can be analyzed spectrophotometrically (optical, Raman) at the point where they are discharged from the cell or collected for other instrumental (epr) or chemical analyses.

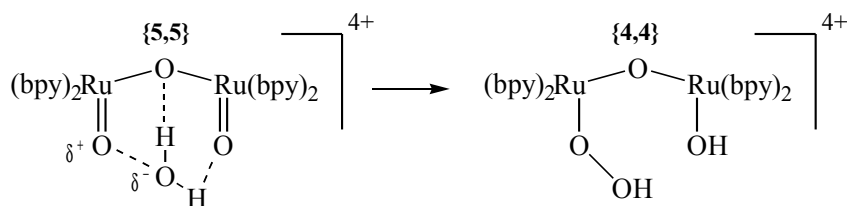
The capability of preparing pure solutions of the μ -oxo dimer in its various oxidation states had previously enabled us to establish that: (i) in 0.1-1.0 M $\text{CF}_3\text{SO}_3\text{H}$ solutions, the accessible oxidation states of the μ -oxo dimer correspond to formal oxidation states on the ruthenium centers of {3,3}, {3,4}, {4,4}, and {5,5}, with {4,5} apparently being unstable with respect to disproportionation; (ii) the {5,5} ion is structurally unique in possessing coordinated oxo atoms in the *cis*-aqua positions and is the only oxidation state kinetically competent to be the O_2 -evolving species; and (iii) the bridging O atom does not undergo exchange with solvent during catalytic turnover. The significance of this last point is that it establishes that the O atoms in the catalyzed reaction are derived solely from the *cis*-coordinated aqua ligands and/or solvent H_2O .

During the current funded period, we sought to identify using ^{18}O -isotopic labeling the pathways by which O_2 is formed. Proper experimental design required knowledge of the *cis*-aqua water exchange rates for the various oxidation states, which

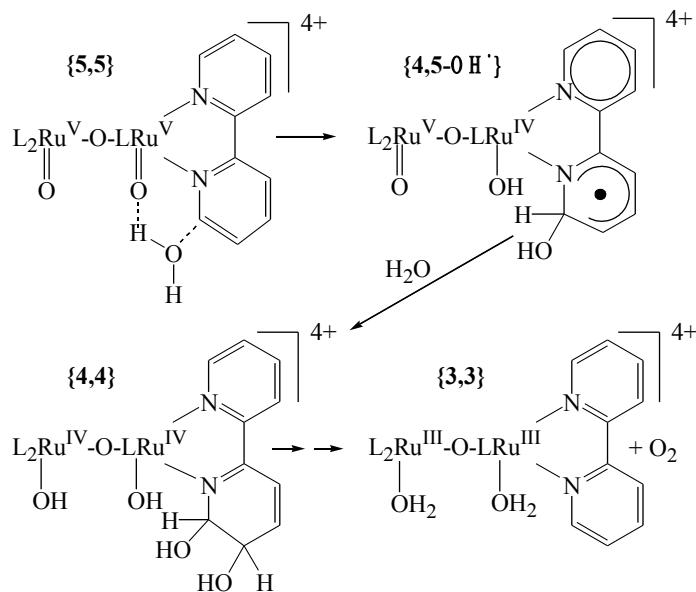
were determined by incubating mixtures of {3,3} and {3,4} ions that were ^{18}O -enriched in the *cis*-aqua positions, then at timed intervals oxidizing portions completely to {5,5} with excess Ce^{4+} ion using a flow-mixer and analyzing the isotopic distribution by resonance Raman spectroscopy (*manuscript 2*). This method takes advantage of the large isotopic shift in ruthenyl stretching modes ($\Delta\nu_s = 38\text{ cm}^{-1}$) for $\text{Ru}=\text{}^{16}\text{O}$ and $\text{Ru}=\text{}^{18}\text{O}$ ions. By measuring the rate of $\text{Ru}=\text{}^{18}\text{O}$ to $\text{Ru}=\text{}^{16}\text{O}$ conversion in the {5,5} ions, we were able to determine that $k_{\text{ex}} = 7 \times 10^{-3}\text{ s}^{-1}$ for water exchange on {3,3} at 23 °C (corresponding to $t_{1/2} = 99\text{ s}$) and to establish that the exchange rates for all higher oxidation states were slow with respect to the rate of catalyzed water oxidation. Thus, oxidation of {3,3} to {3,4} effectively blocked water exchange, yielding stable solutions of substitution-inert ions with a defined isotopic composition of coordinated water.

Earlier isotope-labeling studies from our lab and that of Meyer gave similar, but quantitatively conflicting data; in particular, their data suggested the existence of a bimolecular pathway involving reaction between two coordination complexes, whereas our data gave no evidence for this type of pathway, but indicated that O_2 formation involves a single catalyst ion. To resolve this issue, we designed an experimental system that allows continuous mass spectrometric monitoring of the O_2 product (*manuscript 4*). From the data obtained, it is clear that there are no bimolecular pathways; however, two unimolecular pathways were identified, in which O_2 is formed from either (i) one coordinated terminal ruthenyl $\text{Ru}=\text{O}$ atom in the complex plus one solvent O atom or (ii) two solvent O atoms. From deuterium kinetic isotope measurements made upon the catalytically active form of the complex, we have established that the primary H(D)-isotope effect for water oxidation is anomalously small ($\text{KIE} = 1.6\text{-}1.7$) for ruthenyl-

catalyzed oxidations. From these results and thermodynamic considerations, we have proposed reaction mechanisms that feature addition of H₂O to the complex to form “covalent hydrates”. Specifically, as illustrated below, in the first proposed pathway, OH and H are added in a concerted reaction to adjacent terminal ruthenyl O atoms of the catalyst and, in the second pathway, the OH fragment is added to a bipyridine ring as H is abstracted by one of the ruthenyl O atoms. The relative contribution of pathway *ii* (*hypothetical pathway i*):

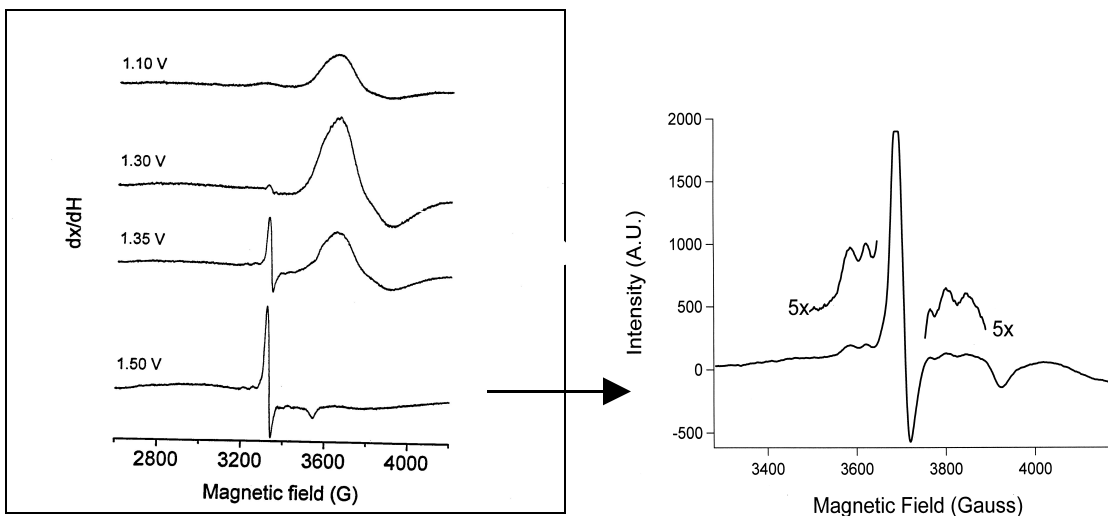


(*hypothetical pathway ii*):



increased from ~45% to ~65% over the temperature range of 10-47 °C. As illustrated, the reactions imply the existence of two distinct mechanisms; however, as discussed in *manuscript 4*, the data do not allow exclusion of a mechanism involving slow formation

of a common intermediate that partitions by two separate pathways to give $^{32}\text{O}_2$ and $^{34}\text{O}_2$. One should note that precedents exist in the chemical literature for each of the proposed steps in the two pathways shown; this aspect is discussed in *manuscript 6*. Furthermore, recent *ab initio* calculations provide support for pathway *i* in confirming the terminally bound Ru hydroperoxy species as a plausible intermediate along a low-energy reaction coordinate leading to O_2 formation (*Mu-Hyun Baik (Indiana University), personal communication, [4]*); the calculated activation free energy for this reaction (26 kcal/mol) was in reasonable agreement with our measured overall apparent activation free energy of 21 kcal/mol at 23 °C (*manuscript 4*) for O_2 formation from {5,5}. Our suggested pathway *ii* invokes formation of ligand radical species as intermediates. As shown in the following figures, cryogenic epr studies provide evidence that appears consistent with this suggestion (*manuscript 6*). Specifically, a relatively sharp $g \sim 2$ axial signal appears

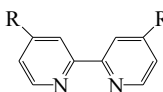


upon electrochemical oxidation to the {5,5} state that is quite unlike the broad rhombic signal observed for the ruthenium {3,4} μ -oxo dimer in its odd-spin paramagnetic state (*left panel*) and other similar dimeric ruthenium ions. No epr signal would be expected

for coupled d^3 Ru(V) centers in **{5,5}**, which would give rise either to a diamagnetic or even-spin paramagnetic ground states. The axial symmetry indicates that the signal must be associated with the coordination complex, i.e., is not adventitiously oxidized organic material, a conclusion which is supported by observations that the intensity (as measured by the amplitude of the g_{\perp} component) increases linearly with the **{5,5}** concentration (data not shown). Furthermore, the g_{\perp} component exhibits a 6-line spectrum that constitutes $\sim 20\%$ of the total signal intensity (*right panel*); this splitting likely arises from hyperfine coupling to individual ^{99}Ru and ^{101}Ru centers, which are the only Ru isotopes that possess nuclear magnetic moments (appropriately, $I = 5/2$) and, collectively, are present at $\sim 30\%$ natural abundance. All of these properties are consistent with the species giving rise to the signals being ligand-centered radicals. A rough estimate of the spin density of this signal made by comparing doubly integrated intensities for the **{3,4}** and **{5,5}** states suggests that $\sim 10\%$ of the **{5,5}** ion is paramagnetic, implying that relatively high concentrations of the radical intermediates accumulate during steady-state decay of the **{5,5}** ion.

b. Ongoing Studies

A series of symmetrically-substituted 2,2'-bipyridine compounds have been synthesized that bear electron-donating or electron-withdrawing substituents, primarily at the ring 4,4'-positions, i.e.,



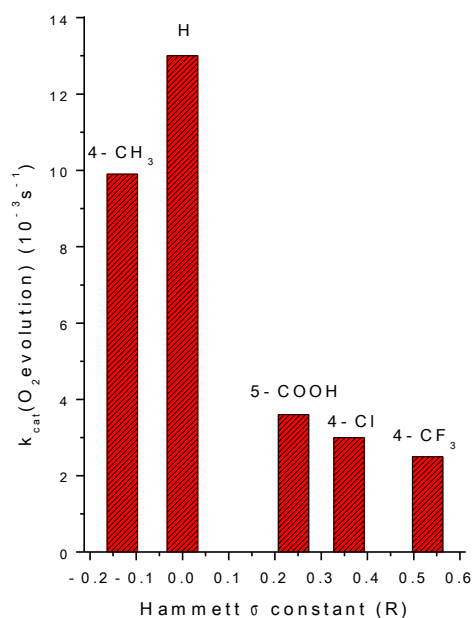
The compounds presently available include

the following (in order of increasing electron-donating character): $R = -\text{CN} < -\text{CF}_3 <$

$-\text{NO}_2 < -\text{NH}(\text{CH}_3)_2^+ < -\text{Cl} < (-\text{H}) < -\text{CH}_3 < -\text{OCH}_3 \approx -\text{O}(\text{CH}_2\text{CH}_2\text{O})_n\text{CH}_3$ ($n = 1-4$) $< -\text{N}(\text{CH}_3)_2$. These will be used as ligands for ruthenium μ -oxo dimers to probe reaction mechanisms. The rationale for these experiments is discussed in the Renewal Proposal; briefly, they should allow systematic variation in the thermodynamic potentials for the various oxidation states and sterically hinder “covalent hydration” to the ring as envisioned in pathway *ii*, with a consequent alteration of various measurable reaction parameters such as overall O_2 evolution rates, rate constants for decay of various oxidation states, partitioning of $^{32}\text{O}_2$ and $^{34}\text{O}_2$ products in isotope labeling experiments, and concentrations of epr-detectable and optically detectable intermediates. Additionally, they will be used in “combinatorial” approaches to preparing asymmetric μ -oxo dimers to test the hypothesis that catalysis rates are greater if the reaction center contains “push-pull” electronic asymmetry. Preliminary data (obtained for a limited set of symmetrical μ -oxo dimers) displaying overall rate constants of O_2 evolution in the presence of excess Ce^{4+} is shown in the adjacent figure.

To understand why the rate constants appear to maximize at the underivatized ligand will require extensive characterization of each of the reactions, as well as extending the data set to include substituents with stronger electron-withdrawing and (particularly) electron-donating character.

We also anticipate initiating structural characterization in the coming

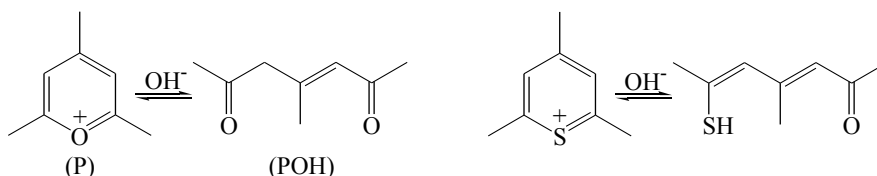


months of the epr-active species observed in {5,5}-containing solutions by ENDOR spectroscopy (in collaboration with Dr. Michael Bowman at Pacific Northwest National Laboratories). These studies should allow us to distinguish among ligand radical species and other recently proposed radicaloid species involving just the O=Ru-O-Ru=O core (*Mu-Hyun Baik (Indiana University), personal communication, [4]*).

3. Photoproduction of H_2 (objective 2)

a. Published work (manuscript 3)

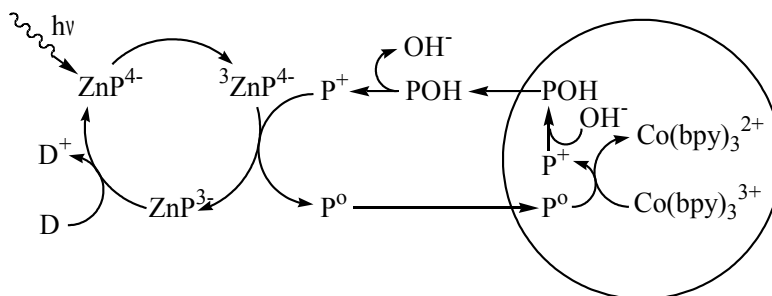
Pyrylium ions and their congeners undergo reversible ring-opening pseudo-base formation, e.g.:



to give the corresponding 1,5-diketones and tautomeric 1,5-thiogluconic aldehydes.

These compounds are also efficient oxidative quenchers of photoexcited sensitizer dyes.

We recently discovered ([5], *manuscript 3*) that these properties could be exploited to develop cyclic transmembrane redox systems in which the pyrylium ion functions both as an oxidative quencher and a cyclic electroneutral transmembrane e^-/OH^- antiporter. The basic photochemical system investigated is diagramed below:



Generic scheme for pyrylium-mediated e^-/OH^- antiport

Major findings from these studies are summarized below:

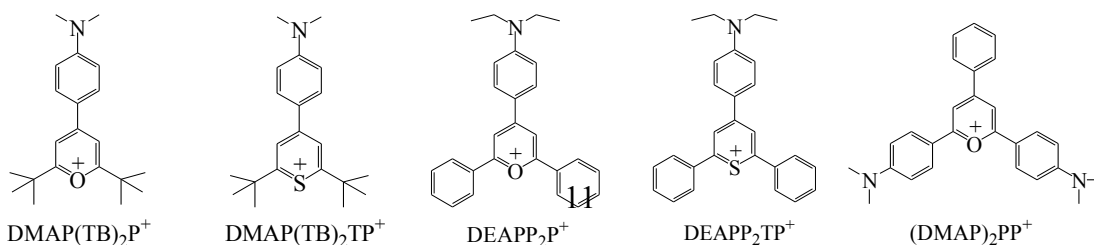
- i.* One-electron transmembrane photoreduction of occluded $\text{Co}(\text{bpy})_3^{3+}$ required the presence of a pyrylium salt, which was shown by transient spectrophotometry to efficiently oxidize the $^3\text{ZnTPPS}^{4-}$ ion.
- ii.* From comparison of the measured permeabilities of P^+ , H^+ , and P^0 with overall transmembrane redox rates, it was evident that P^0 was the electron carrier. Each electron carrier was demonstrated to transport up to 200 electrons (i.e., cycle 200 times), at which point the internal pool of electron acceptors ($\text{Co}(\text{bpy})_3^{3+}$) was exhausted.
- iii.* Overall quantum yields with P^+ as oxidative quencher were $\phi \sim 0.2$; POH could also oxidize $^3\text{ZnTPPS}^{4-}$, although with quenching rate constants that were ~ 5 -fold lower than for P^+ . From the known ϕ values for individual steps, it was calculated that transmembrane electron transport occurred with near-unitary efficiency.
- iv.* Direct photoexcitation of P^+ in vesicle assemblies lacking added sacrificial electron donors also led to net photoreduction of occluded $\text{Co}(\text{bpy})_3^{3+}$.

Photoexcited pyrylium and thiopyrylium ions are strongly oxidizing; presumably, the source of electrons for this reaction was either solvent or buffer components. The apparent simplicity of this reaction, in which the pyrylium functions both as photosensitizer and cyclic redox carrier, is appealing with respect to potential technological applications. The lowest energy absorption bands of the pyrylium ions used in these studies were in the near-uv region, however, requiring that other similarly-functioning pyrylium analogs be found that absorb visible photons.

b. Ongoing studies

The aqueous one-electron reduction potential for 2,4,6-trimethylpyrylium ion (TMP^+) is $E^\circ = -0.44 \text{ V}$ (vs NHE). In principle, this driving force is sufficient to reduce H^+ to H_2 in weakly acidic solutions (e.g., $E^\circ(2\text{H}^+/\text{H}_2) = -0.30\text{V}$ at pH 5). Liposomal systems were prepared in which colloidal Pt was generated *in situ* in place of $\text{Co}(\text{bpy})_3^{3+}$ in the inner aqueous compartment by reduction of H_2PtCl_6 with H_2 . Transmission electron micrographs confirmed the formation within the vesicles of a Pt colloid whose average particle size was $\sim 5 \text{ nm}$. Although initial studies using a Pt-loaded PC liposomal assembly with electron donors, ZnTPPS^{4-} , and TMP^+ in the external medium indicated formation of H_2 under continuous photolysis, we have not been able to reproduce these results. It now seems likely that observed reaction was catalyzed by Pt located in the external medium; ZnTPPS^{4-} -initiated photoproduction of H_2 is efficient under these conditions in the absence of vesicles.

We have recently synthesized a series of analogous pyrylium and thiopyrylium salts which contain electron-donating substituents that both lower the intrinsic reduction potentials and shift their optical absorption bands into the visible spectral region. These compounds are being used to determine if the pyrylium-photosensitized system (item *iv*, previous section) can be driven by solar photons and if problems with the Pt-catalyzed H_2 photoproduction systems can be overcome by increasing the thermodynamic driving force for electron transfer from the Py^0 donor. Among the compounds synthesized, the following have been extensively characterized:



Relevant physical and chemical properties of these ions that we have determined are collected in the following table:

Pyrylium ion	λ_{\max} (nm) ^a	$E_{1/2}(P^{+/0})$ (V) ^b	pK _a ^c	ϕ (Co(bpy) ₃ ²⁺) ^d
DMAP(TB) ₂ P ⁺	492	-1.1	5.5	0.026
DMAP(TB) ₂ TP ⁺	530	-0.96	7.0	0.032
DEAPP ₂ P ⁺	545	-0.89	5.5	0.016
DEAPP ₂ TP ⁺	588	-0.76	6.8	0.026
(DMAP) ₂ PP ⁺	612	-1.0	5.6	0.014

^ain 1:1 (v/v) CH₃CN/water; ^bby cyclic voltammetry in dry CH₃CN vs. Ag/0.1 M AgNO₃ (DMSO); ^cpseudo-acid dissociation constant, defined as $K_a = [H^+][POH]/[P^+] = K_w/K_b$, with K_b defined as the pseudo-base dissociation constant, measured spectrophotometrically in 1:1 (v/v) CH₃CN/40 mM aqueous sodium acetate; ^doverall quantum yields from continuous photolysis at 420 nm (Soret maximum) of 5 mg/mL suspensions of PC vesicles in 40 mM Tris/Cl, pH 8.0, containing 25 μ M occluded Co(bpy)₃³⁺ and 2 μ M pyrylium ion, with 2 μ M ZnTPPS⁴⁻ and 5 mM EDTA in the external medium.

Continuous photolysis under a wide range of conditions using either the ZnTPPS⁴⁻ photosensitization system (e.g., Table 1, column 5) or direct photoexcitation of the pyrylium dyes with visible light led to net transmembrane reduction of Co(bpy)₃³⁺ in PC vesicle assemblies, demonstrating that each of these compounds could function as combined photosensitizer/transmembrane redox carriers. However, in no instance have we yet achieved photosensitized H₂ reduction with vesicles containing occluded Pt particles.

To better characterize the redox behavior of the pyrylium radicals, we have initiated studies of their reactivities toward a series of viologens whose one-electron reduction potentials are comparable to those of the pyrylium ions. Studies to date have used primarily N,N'-dimethyl-4,4'-bipyridinium (methyl viologen, MV²⁺), the corresponding benzyl derivative (BV²⁺), and a o-xylyl-linked cofacial diviologen (DV⁴⁺); reduction potentials for these ions under the same conditions determined for the pyrylium ions (see Table) are $E_{1/2}(MV^{2+/+}) = -0.73$ V, $E_{1/2}(BV^{2+/+}) = -0.62$ V; and $E_{1/2}(DV^{4+/3+}) =$

-0.45 V. Consequently, if the relative homogeneous potentials accurately reflect the potentials in the microphase environment of the PC liposome, the pyrylium radicals are thermodynamically capable of reducing all of the viologens to their corresponding radical cations. We have found that DV⁴⁺ occluded within PC liposomes readily undergoes pyrylium-mediated reduction to the corresponding DV³⁺ radical during continuous photolysis of ZnTPPS⁴⁻ in the sacrificial donor system; in this reaction, the efficiencies of each of the derivatized pyrylium ions appear to be similar, with overall quantum yields of $\phi \sim 0.01$. However, reduction of the lower-potential viologens has not yet been achieved. The reason for this unreactivity is uncertain, although one contributing factor may be that extrapolation of redox potentials measured in homogeneous solution is inappropriate for vesicle assemblies. In vesicles, the reduction potential of pyrylium ion may be significantly raised by stabilization of the neutral radical in the lipophilic interior of the membrane, whereas the viologen potentials would be relatively lower since the cationic viologen radicals partition preferentially within the hydrophilic aqueous regions of the assembly.

Transient spectrophotometric and multi-mixing flow kinetic experiments designed to characterize individual reaction steps and thereby improve our understanding of the reactivities of pyrylium ions in these assemblies are in progress. The combined results of these studies will be published as *manuscript 10*.

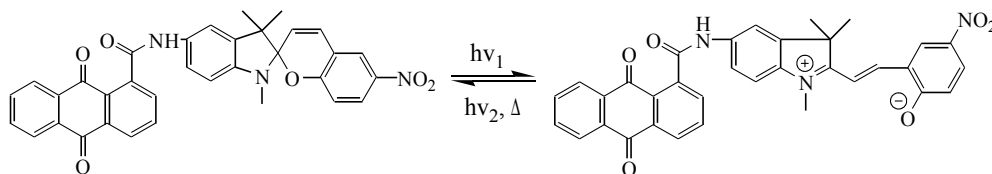
4. *Light-modulated Transmembrane Redox (objective 3)*

a. Published Work (manuscripts 1,5,7-9).

Among the various mesoscopic particles that are used as organizing matrices for controlling chemical reactivity, vesicles have the unique capacity to store energy in the

form of electrochemical gradients across their closed bilayer membranes. In this sense, redox-active vesicle assemblies that generate transmembrane potentials mimic the energy-transducing capabilities of living cells. The systems developed by the Gust, Moore and Moore group utilizing artificial donor-sensitizer-acceptor triads as liposomal electron transport chains coupled to a membrane-localized quinone pool to generate a photoinitiated proton motive force [6] are now classical examples of this “biomimetic” approach to solar energy photoconversion. Nonetheless, the transmembrane redox mechanisms functioning in these systems are totally unlike biological Q-cycles. These contain quinone-binding sites at alternate ends of membrane-spanning electron transport chains at which the quinones undergo two sequential one-electron reductions to the corresponding hydroquinones, or vice-versa. One consequence of this organization is that, unlike the artificial systems, protons are vectorially transported via the Q-QH₂ couple, thereby avoiding accumulation of O₂-reactive semiquinones.

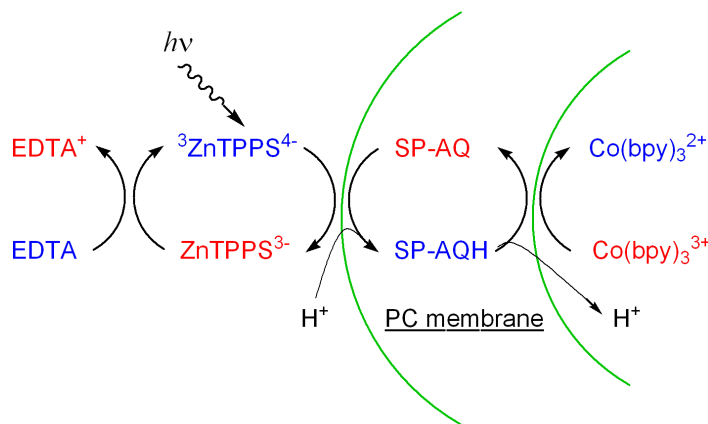
Mechanisms by which the quinone pool mediates transmembrane redox in artificial systems are not well-characterized. To gain insight into these processes, we have coupled a photoisomerizable spiropyran (SP) molecule to anthraquinone (AQ) (*manuscript 8*), the intent being to identify and achieve control of the anthraquinone location within the membrane. As illustrated in the following scheme, ultraviolet illumination induces heterocyclic photocleavage of the C(spiro)-O bond, forming the more polar merocyanine (MC) form of the dye:



Reversible spiro-mero interconversion in a spiropyran-anthraquinone (SP-AQ) conjugate

Based upon our earlier experience with spiropyrans and related compounds ([7], *manuscripts 1,5*), we anticipated that the MC form would localize within a more polar microphase region of the membrane, i.e., closer to the aqueous-organic interface, and undergo transmembrane diffusion at a considerably slower rate.

Transmembrane redox mediated by these SP-AQ compounds was studied using a photoredox system consisting of ZnTPPS^{4-} and the sacrificial electron donor, EDTA, in the bulk aqueous phase of phosphatidylcholine (PC) vesicles containing bound SP-AQ and the electron acceptor, Co(bpy)_3^{3+} , occluded within the inner aqueous compartment, as indicated in the following diagram:



Topographic organization of the photoreaction system, illustrating an electroneutral H^+/e^- cotransport mechanism; the arcs represent the two aqueous-organic interfaces of the closed bilayer membrane.

The photoredox behavior of this system is quantitatively described in *manuscript 8*; major findings are as follows:

- i. Net photoreduction of Co(bpy)_3^{3+} required all system components be present, with oxidative quenching of ZnTPPS^{4-} by the vesicle-bound anthraquinones being the predominant mechanism.
- ii 30-35% photoconversion of the SP moiety to MC caused the net redox quantum yield to decrease by (3-6)-fold; transient spectroscopy and fluorescence

quenching studies revealed that two major factors contributed to this effect, viz., greater fluorescence quenching of $^1\text{ZnTPPS}^{4-}$ by the MC group and lowered transmembrane diffusion by the MC-containing redox shuttles.

- iii* Two different transmembrane redox mechanisms that depended upon the identity of the redox shuttle were revealed by addition of a protonophore (CCCP) or a K^+ -selective ionophore (valinomycin) to the membranes. Specifically, the internal $\text{Co}(\text{bpy})_3^{3+}$ was completely reduced under continuous photolysis when SP(MC)-AQ was the carrier, and addition of ionophores did not affect the photoreaction rate. In contrast, when AQ or a lipophilic SP-AQ analog containing an “anchoring” dodecylphenoxy ($-\text{OC}_6\text{H}_5\text{C}_{12}\text{H}_{25}$) substituent was the carrier, $\text{Co}(\text{bpy})_3^{3+}$ reduction was incomplete unless ionophores were added, and the reaction proceeded in a self-impeding manner characteristic of a developing transmembrane electrical potential. Thus, electron transport by SP(MC)-AQ is electroneutral, most likely occurring by transmembrane diffusion of the SP-AQH semiquinone, whereas this pathway is blocked for AQ and the SP(MC)-AQ dodecylphenoxy derivative. The latter reactions occurred by net translocation of charge, the most likely mechanism being transbilayer electron exchange between AQ and AQ^- , since transmembrane permeabilities of lipophilic anions are generally many orders of magnitude less than for the corresponding neutral molecules. The basis for the differing mechanisms may be the relative locations of the carriers; AQ and SP-AQ- C_{12} are located more deeply within the hydrocarbon phase of the membrane where access to protons should be restricted.

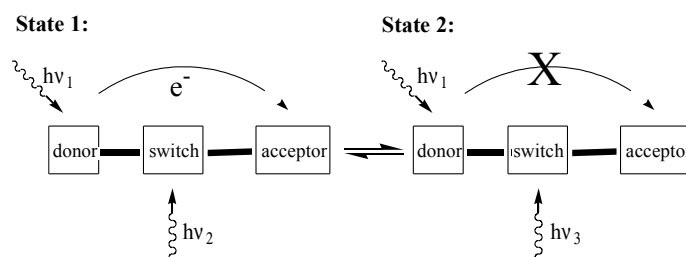
Manuscripts 1 and 5 are involved with examining the effects of spiro-mero interconversion on passive electrolyte leak rates across unilamellar vesicle membranes. We found that the SP \rightarrow MC conversion decreased the leak rate of K^+ from the membrane interior (*manuscript 1*), an observation that allowed us to interpret solvatochromic shifts in the MC absorption band observed for transient spectra following photoisomerization [7] as arising from relocation of the dye from the membrane interior toward the aqueous-organic interface. This conclusion was reinforced by appending a K^+ -selective crown ether to the dye. In this case, the relative leak rate was reversed, with MC-crown conjugate being more effective than the SP-crown (*manuscript 5*). Presumably, whereas the interfacially located MC-crown conjugate had access to aqueous K^+ ions and could thereby function as a K^+ uniporter, the crown was restricted from the interface when the dye was in its hydrophobic SP form. The behavior observed for these spiropyran systems is totally consistent with that of the SP-AQ conjugates described above.

During the course of our work on SP-elicited light modulation of membrane organized systems, the opportunity arose to use some of our compounds in novel materials applications. In collaboration with Dr. Alexander Li's group, we developed SP(MC)-conjugated CdSe/ZnS nanocrystalline particles whose intrinsic intense fluorescence could be switched off by fluorescence energy transfer (FRET) when the conjugated dye was in its merocyanine form (*manuscript 7*). We also developed polymeric organic hybrid nanoparticles which provided an environment in which the MC form of the dye was highly fluorescent (*manuscript 9*). This is exceptional because MC is virtually nonfluorescent in most environments. As described in the papers, numerous

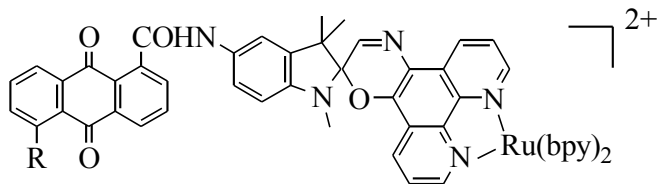
applications in molecular electronics, data storage, and biomolecular tagging can be envisioned.

b. Ongoing Studies.

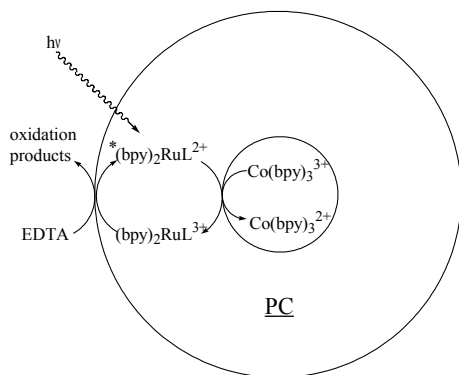
Within the broader issue of the limits to which biomimetic systems can parallel bioenergetics, we have been interested in developing bifunctional artificial systems in which electrogenic transmembrane redox is regulated by controlling transmembrane potentials, analogous to electron transport in mitochondria and chloroplasts. To date, our experimental designs have involved using photoisomerizable dyes and electrogenic transmembrane redox systems as separate elements. One major problem that we have encountered is that these elements often cross-react, i.e., diffusible redox intermediates irreversibly oxidize the dyes that are intended to function as ion gates. (This problem is avoided, of course, in biological organelles by sequestering the redox components within protein matrices.) Consequently, we have designed single molecules to contain both ion gating and electron transport functions, viz.:



and have recently synthesized one such molecule, shown below:



where R = H or $-\text{OC}_6\text{H}_5\text{C}_{12}\text{H}_{25}$ (4-dodecylphenoxy). Preliminary studies indicate that these ions mediate transmembrane redox upon excitation of the Ru chromophore in PC liposomal assemblies similar to those described for SP-AQ (*manuscript 8*), i.e.,



Based upon our experience with similar membrane-doped spiro compounds ([7], *manuscripts 1,5,8*), we anticipate that the phenanthroline-type spirooxazine incorporated into this triad will function to modulate transmembrane redox at two levels. First,

reversible photoisomerization at the spiro carbon to an open-ring merocyanine form substantially increases pseudo- π conjugation between the indolene and oxazine segments of the spirooxazine unit, and may thereby increase electron transfer efficiencies between the donor and acceptor groups appended to the opposite segments. Second, if constrained to the membrane interior, photoconversion to the merocyanine form should disrupt the normal membrane bilayer structure and increase electrolyte leak rates. This, in turn, would dissipate transmembrane potentials that accompany electrogenic transmembrane redox, increasing the thermodynamic driving force and, correspondingly, the rates of electron transport.

One potential problem involving switching in this system is that coordination of the $-\text{Ru}^{\text{II}}(\text{bpy})_2$ moiety to these ligands gives complexes that are entirely in the SP isomeric form. Flash excitation at 355 nm causes partial conversion to the MC form, but thermal ring closing rapidly ensues, with $t_{1/2} \sim 10\text{-}100$ ms. We have attributed these effects to the extensive ground-state $d_\pi \rightarrow \text{L}$ backbonding that is characteristic of Ru^{II}

complexes [7]. Thermal ring closing in the vesicles is slowed 10^2 -fold for the dodecylphenoxy-derivatized ligand, perhaps reflecting packing constraints by the ordered alkyl chains of the surfactant. Use of other photoreactive metal centers, specifically, $\text{-Re}(\text{CO})_3\text{Cl}$, may also give more tractable $\text{SP} \rightarrow \text{MC}$ equilibria and dynamics.

5. Cited Literature

- [1] “Basic Research Needs for Solar Energy Utilization”, Report of the Basic Energy Sciences Workshop on Solar Energy Utilization, April 18-21, 2005
(http://www.sc.doe.gov/bes/reports/files/SEU_rpt.pdf).
- [2] J. A. Gilbert, D. S. Eggleston, W. R. Murphy, Jr., D. A. Geselowitz, S. W. Gersten, D. J. Hodgson, & T. J. Meyer: “Structure and Redox Properties of the Water- Oxidation Catalyst $[(\text{bpy})_2(\text{OH}_2)\text{RuORu}(\text{OH}_2)(\text{bpy})_2]^{4+}$ ”, *J. Am. Chem. Soc.* **1985**, *107*, 3855-3864.
- [3] H. Yamada & J. K. Hurst: “Resonance Raman, Optical Spectroscopic, and EPR Characterization of the Higher Oxidation States of the Water Oxidation Catalyst, *cis,cis*- $[(\text{bpy})_2\text{Ru}(\text{OH}_2)]_2\text{O}^{4+}$ ”, *J. Am. Chem. Soc.* **2000**, *122*, 5303-5311.
- [4] M.-H. Baik & X. Yang: “Theoretical Study of the Mechanism of Water Oxidation Catalyzed by the *cis,cis*- $[(\text{bpy})_2\text{Ru}(\text{OH}_2)]_2\text{O}^{4+}$ Ion”, Abstracts of Papers (INOR-470), 230th ACS National Meeting, Aug. 28-Sept. 1, **2005**, Washington, D.C.; X. Yang & M.-H. Baik: “Electronic Structure of the Water-Oxidation Catalyst, $(\text{bpy})_2(\text{OH}_x)\text{RuORu}(\text{OH}_y)(\text{bpy})_2]^{z+}$: Weak Coupling between Metal-Centers is Preferable over Strong Coupling”, Abstracts of Papers (INOR-476), 230th ACS National Meeting, Aug. 28-Sept. 1, **2005**, Washington, D.C.

- [5] R. F. Khairutdinov & J. K. Hurst: “Cyclic Transmembrane Charge Transport by Pyrylium Ions in a Vesicle-based Photocatalytic System”, *Nature* **1999**, 402, 509-511.
- [6] G. Steinberg-Yfrach, P. A. Liddell, S. C. Hung, A. L. Moore, D. Gust & T. A. Moore: “Conversion of Light Energy to Proton Potential in Liposomes by Artificial Photosynthetic Reaction Centres”, *Nature* **1997**, 385, 239-241; G. Steinberg-Yfrach, J.-L. Rigaud, E. N. Durantini, A. L. Moore, D. Gust & T. A. Moore: “Light-driven F₀F₁-ATP Synthase-catalyzed Production of ATP by an Artificial Photosynthetic Membrane”, *Nature* **1998**, 392, 479-482.
- [7] R. F. Khairutdinov, K. Giertz, J. K. Hurst, E. N. Voloshina, N. A. Voloshin & V. I. Minkin: “Photochromism of Spirooxazines in Homogeneous Solution and Phospholipid Liposomes”, *J. Am. Chem. Soc.* **1998**, 120, 12707-12713.

C. Personnel:

- (1) James K. Hurst, Principal Investigator
12.5 % time (04/01/02-present)
- (2) Rafail F. Khairutdinov, Sr. Research Associate
100% time (05/03/02-10/15/02; 07/15/04-01/01/05)
- (3) Hiroshi Yamada, Visiting Scientist
50% time (07/01/02-09/01/02)
- (4) Linyong Zhu, Postdoctoral Research Associate
100% time (12/03/03-present)